[Article ID] 1003- 6326(2002)04- 0561- 08

Changes in lamellar microstructure by parallel twinning during creep in soft PST crystal of TiAl alloy①

H. Y. Kim, K. Maruyama
(Department of Material Science, Graduate School of Engineering,
Tohoku University, 02 Aobayama, Sendai 980-8579, Japan)

[Abstract] Compression creep tests of a Ti-48% Al (mole fraction) alloy were carried out at 1 150 K with soft-orientated PST crystal. Parallel twinning took place during the creep. Changes in lamellar microstructure caused by the parallel twinning were investigated, and their effects on creep deformation behavior were discussed. The results show that the parallel twinning occurs in an early stage of creep, and makes significant contribution to creep strain in the domains favorably oriented for the twinning. The nucleation of parallel twins finishes at a strain of about 3%. There is a critical resolved shear stress for parallel twinning, and it is about 50 MPa in the Ti-48% Al PST crystals at 1 150 K. The activity of parallel twinning increases with increasing applied stress or in a coarse lamellar material. The addition of parallel twins reduces the average value of lamellar spacing. In general, the refinement of lamellar structure should improve creep resistance. However the strengthening by parallel twinning is not evident in creep of the soft PST crystals because the soft deformation modes are the dominant deformation mode in the crystals.

[Key words] titanium aluminide; intermetallics; lamellar microstructure; creep; twinning
[CLC number] TG 146.2 [Document code] A

1 INTRODUCTION

TiAl-based alloys are a prospective light material for high temperature structural applications such as automotive and aerospace engine component, and have been investigated extensively in the last decade[1, 2]. TiAl alloys consist of γ-TiAl and α_2-Ti_3Al phases, and take several types of microstructures depending on their heat treatment. Among those microstructures, a fully lamellar structure is the most favorable for the high temperature applications owing to their superior creep resistance, fracture toughness and fatigue resistance[3~9]. It has been well established that the morphology of lamellar structure strongly influences creep properties of TiAl alloys[9, 10]. It should also be noted that the lamellar structure usually changes during creep at elevated temperature. To design the lamellar structure properly, the microstructural changes during creep and their influence on creep properties should be understood.

The following events are the representative changes that occur during creep exposure of lamellar TiAl alloys: 1) decrease in α_2 volume fraction by dissolution of thin α_2 lamellae or precipitation of γ plates in thick α_2 lamellae; 2) spheroidization of lamellae; 3) parallel twinning.

The precipitation of γ plates and parallel twinning result in refinement of lamellar structure and the consequent strengthening. On the other hand, the dissolution of α_2 lamellae eliminates α_2/γ boundaries, and coarsens lamellar structure. The coarsening and spheroidization of lamellar structure brings about weakening of TiAl alloys. This paper focuses on the parallel twinning among the three microstructural changes.

Plastic deformation of TiAl alloys can occur by mechanical twinning associated with $1/6\langle 112]\{111\}$ shearing[11, 12]. In this paper, (111) plane is defined to be parallel to lamellar boundaries. Twinning on this type of planes introduces additional γ plates parallel to the original lamellae, and is called parallel twinning. There is only one true twinning direction $\boldsymbol{b} = 1/6[11\bar{2}]$ on (111) plane since the other $1/6\langle 112]$ displacements destroy the ordered $L1_0$ structure of TiAl. Mechanical twinning in TiAl alloys has been observed during superplastic and creep deformation[13~19]. It has been suggested that the contribution of mechanical twinning should be considered when analyzing creep deformation of TiAl alloys[11]. Mechanical twinning mechanisms in TiAl alloys have been well understood in the last few years[20, 21]. However, details of parallel twinning during creep and the contribution to creep strain are not clear at present. It has been reported that the activity of mechanical twinning depends on stress, temperature and strain[14, 19, 22, 23]. It is also needed to clarify the effect of the deformation conditions on the activity of parallel twinning.

In this study, evolution of the parallel twins and the consequent lamellar refinement during creep are quantitatively investigated with soft-orientated PST

① [Received date] 2001- 10- 08

crystal of a Ti-48% Al (mole fraction) alloy. The contribution of parallel twinning to creep strain is analyzed, and the effect of lamellar refinement on creep behavior is discussed. More details have been reported elsewhere[24].

2 EXPERIMENTAL

The PST crystal of TiAl alloy used in the present study was grown at Kyoto University with a growth rate of 1.4×10^{-7} m/s. Its nominal composition is Ti-48% Al (mole fraction). Compression specimens, 2 mm × 2 mm in cross section and 3 mm in height, were cut from the as-grown PST crystal. The orientation of compression specimens is schematically drawn in Fig. 1. One of the surfaces of the parallel piped is $\{11\bar{2}\}$, and the lamellar boundaries are parallel to (111). The angle between lamellar boundaries and the stress axis was controlled to be 35°. The specimens were subjected to creep tests without applying any other heat treatment. Table 1 gives the compression axes of the six orientation variants of lamellae in accordance with the notation of Inui et al[13].

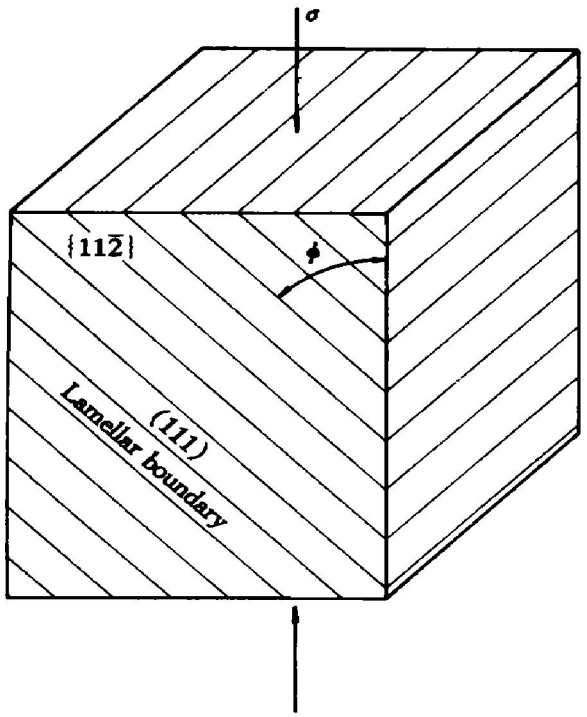

Fig. 1 Schematic drawing of soft-oriented PST crystal

Compression creep tests were conducted under constant stress condition at applied stresses ranging from 100 to 400 MPa. The testing temperature of 1 150 K was kept within ±1 K during creep tests. Specimens were protected from oxidation by an argon gas atmosphere. Creep tests were terminated at strains of 2%, 5% and 20% at a constant stress of 251 MPa to investigate the evolution of parallel twinning. Another series of creep tests were terminated after a strain of 5% to investigate the effect of applied creep stress on the twinning. The specimens were cooled down to room temperature at an initial cooling rate of 0.25 K/s under full load in order to retain the deformation microstructures. Thin foils for transmission electron microscopy (TEM) were sectioned from the crept specimens, so as to obtain ⟨112⟩ as the foil normal. The thin foils were prepared using a standard twinjet thinning technique. TEM observation was conducted with a JEOL™ EX 2000 transmission electron microscope operated at 200 kV. Lamellar spacing was measured using a number of lamellae: about 150 lamellae in each specimen. An arithmetical average value of lamellar spacing is used without taking account of the type of boundaries (α_2/γ or γ/γ boundaries). Thickness and spacing of α_2 phase were obtained from scanning electron micrographs (SEM) taken by compositional contrast of backscattered electrons.

3 RESULTS AND DISCUSSION

3.1 As-grown microstructure

The as-grown crystal used in the present study has an α_2 volume fraction of 15%. The size distributions of lamellar spacing, α_2 thickness, and α_2 spacing in the present crystal obey a long-normal distribution as known in Ref. [16]. The arithmetical

Table 1 Miller indices of compression axis, and Schmid factors of ⟨110]{111} ordinary slip and [11$\bar{2}$](111) parallel twinning systems in each γ domain

Domain	I_M	I_T	II_M	II_T	III_M	III_T
Compression aixs	$\bar{3}114$	$31\bar{1}\bar{4}$	1143	$\bar{4}31\bar{1}$	$4\bar{3}11$	$\bar{1}\bar{1}43$
[1$\bar{1}$0](111)	−0.470	0.470	0.235	0.235	0.235	0.235
[1$\bar{1}$0](111)	−0.157	0.157	0.352	−0.196	−0.196	0.352
[110]($\bar{1}$11)	0.403	−0.224	−0.419	0.011	0.011	−0.419
[110](1$\bar{1}$1)	−0.024	0.403	0.618	0.050	0.050	0.168
[11$\bar{2}$](111)	0	0	0.407	−0.407	−0.407	0.407

M—matrix; T—twin

average lamellar spacing of the as-grown crystal was 513 nm, with average α_2 thickness and spacing of 410 nm and 2.7 μm, respectively.

Glide of ordinary 1/2⟨110] dislocation on {111} planes and 1/6⟨112]{111} twinning are the primary deformation modes operative during creep of the soft-oriented PST crystal at 1150 K[25]. Schmid factors for the ordinary slip and parallel twinning system are listed in Table 1. The parallel twinning is a favorable deformation mode in only two of the six γ domains (domains III_M and II_T) in compression tests. In the other domains compressive stress acts against (II_M and III_T) or does not assist (I_M and I_T) the parallel twinning. The $[1\bar{1}0](111)$ easy mode slip is the dominant deformation mode in the domains I_M and I_T. In the domains II_M and III_T, the $[110](\bar{1}11)$ slip system has the highest Schmid factor. The activity of the $[1\bar{1}0](111)$ soft mode slip has been reported in the domains II_T and III_M in addition to the parallel twinning[25].

3.2 Evolution of parallel twinning during creep deformation

Fig. 2 shows an example of TEM micrographs taken after creep deformation to 5% strain at 251 MPa and 1150 K. The domain *A* contains thin plates running parallel to the original lamellar boundaries. The diffraction pattern indicates that the plates are in twin relation with respect to the matrix. They are terminated at the boundary between the domain *A* and *B*, since the parallel twinning system is unfavorably oriented in the domain *B*. These facts suggest that the thin plates were introduced by parallel twinning during creep. The generation of parallel twins reduces average lamellar spacing. To investigate the evolution of parallel twinning, the lamellar spacing was characterized statistically as a function of creep strain. Fig. 3 illustrate the log-normal distribution of lamellar spacing of as-grown and crept specimens at 251 MPa and 1150 K. The crept specimens show a shift of the distribution curves toward smaller spacing. The shift is significant up to a stain of 2%, but a little after 2% strain. The distribution curves indicate that lamellae with large spacing disappeared while the left end did not move. This fact suggests that the parallel twinning primarily took place in thick γ lamellae but hardly occurred in thin γ lamellae. The refinement of lamellar spacing during high temperature deformation is consistent with previous studies on polycrystalline TiAl alloys[14, 26, 27].

The arithmetical average values of lamellar spacing are plotted as a function of creep strain in Fig. 4. The lamellar spacing decreases significantly up to a creep strain of 2% and remains almost constant after 5% strain. It suggests that the parallel twinning

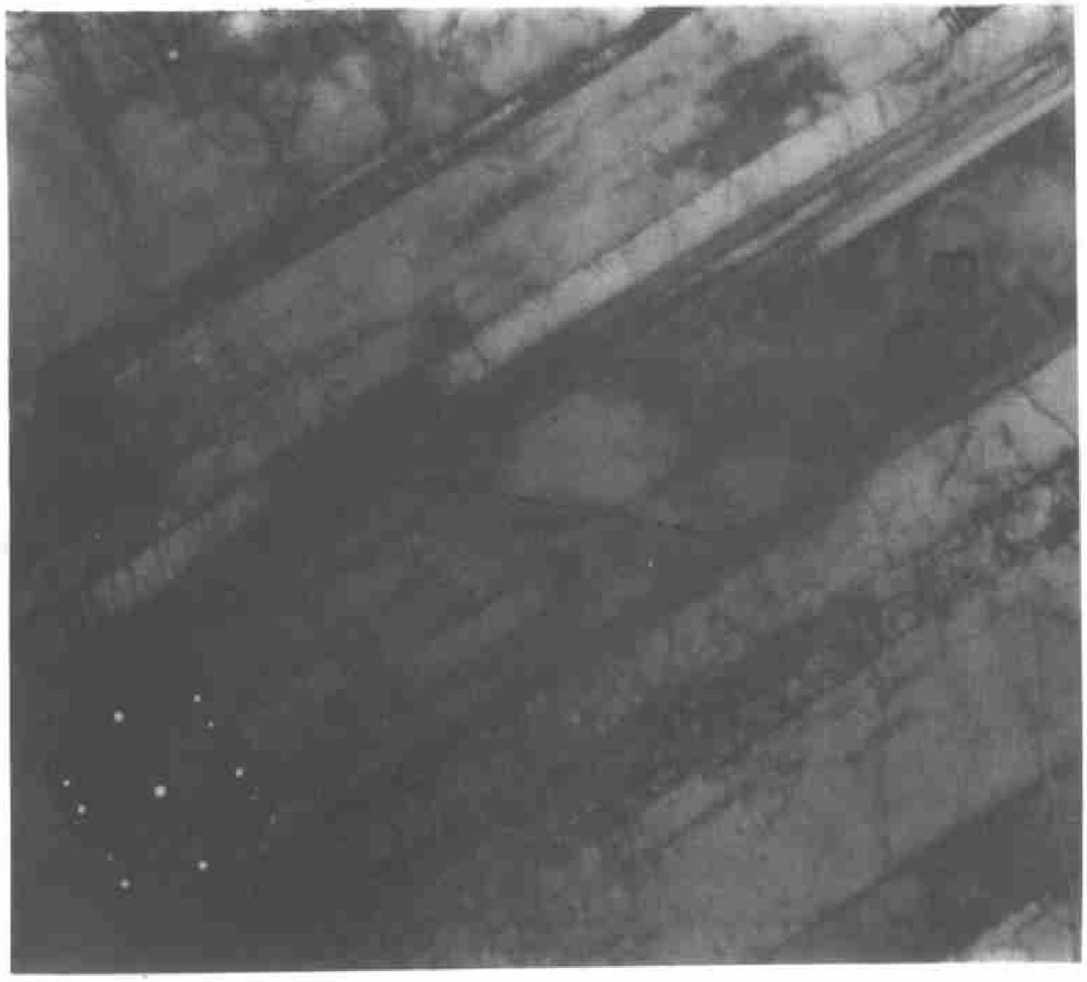

Fig. 2 TEM micrograph of soft-orientated PST crystal deformed at 1150 K and 251 MPa to 5% strain

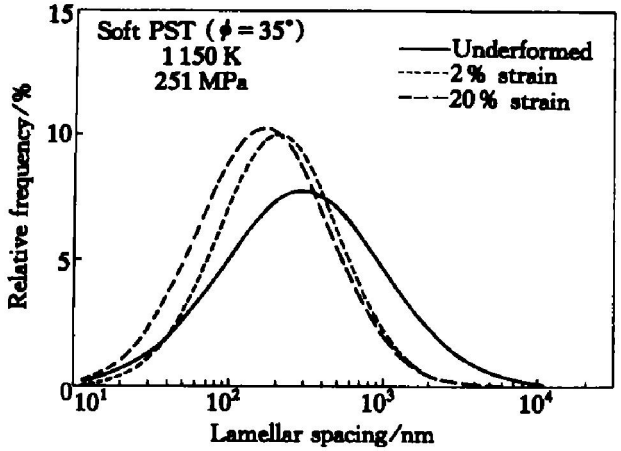

Fig. 3 Change in distribution curve of lamellar spacing with progress of creep deformation at 251 MPa

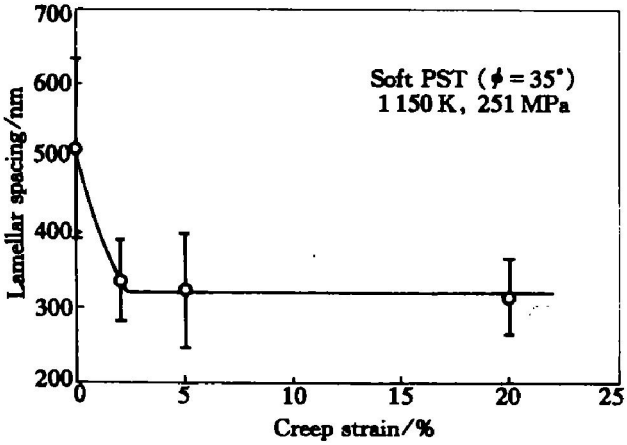

Fig. 4 Change in arithmetical average lamellar spacing λ with creep strain

contributes to deformation in the early stage of creep only. In the later stage, dislocation glide is the dominant deformation mode even in the domain II_T and III_M favorably oriented for parallel twinning. This is in good agreement with the results obtained by Seo et al[26] and Skrotzki et al[14]. In these studies mechanical twinning has finished at a strain less than 1%.

3.3 Contribution of parallel twinning to creep strain

The parallel twinning reduces the average lamellar spacing λ according to the following equation:

$$\frac{1}{\lambda} = \frac{1}{\lambda_0} + 2n \tag{1}$$

where λ_0 is the average value of the initial lamellar spacing, n is the number of parallel twins introduced in a unit length, and $1/\lambda$ corresponds to the number of lamellar boundaries in a unit length.

The parallel twinning creates the following amount of strain:

$$\varepsilon_T = mnt_T \gamma_T \tag{2}$$

where m is the Schmid factor for the parallel twinning, t_T is the average thickness of a parallel twin, and γ_T is the amount of twinning shear that is $1/\sqrt{2}$ in FCC structure. From Eqns. (1) and (2), one obtains

$$\frac{1}{\lambda} = \frac{1}{\lambda_0} + \frac{2\varepsilon_T}{mt_T \gamma_T} \tag{3}$$

The creep strain ε_T caused by parallel twinning can be estimated from the change in the arithmetical average value of lamellar spacing.

The two types of domains are favorably oriented for parallel twinning among the six domain types of lamellae. Suppose all the creep strain is accomplished by parallel twinning in those domains, namely,

$$\varepsilon_T = \varepsilon/3 \tag{4}$$

where ε is the total creep strain. The Schmid factor for the $[11\bar{2}](111)$ parallel twinning is calculated to be 0.407, as shown in Table 1. The average thickness of a twin plate was measured to be 40 nm in the specimen crept to 2% strain at 251 MPa. Fig. 5 illustrates the change in the number of lamellar boundaries ($1/\lambda$) during the creep test at 251MPa as a function of the total creep strain ε. The solid line was estimated with Eqn. (3) on the assumption of Eqn. (4). The estimated line agrees very well with the experimental result. It follows from this fact that the parallel twinning created most of the creep strain of the two favorably oriented domains in the early stage of creep.

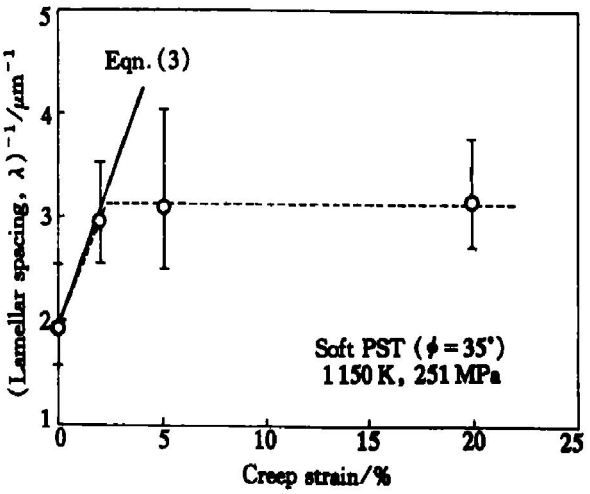

Fig. 5 Reciprocal values of λ plotted against creep strain
(Solid line was estimated with Eqn. (3))

Morris and Leboeuf[21] have estimated the contribution from mechanical twinning to the total creep strain in γ grains of a duplex TiAl alloy: 10% and 50% for 280 MPa and 360 MPa, respectively, at 973 K. This is in good agreement with the present study: 33% at 251 MPa and 1 150 K in the early stage of creep.

3.4 Effect of applied stress on parallel twinning activity

Fig. 6 represents the log-normal distribution curves of lamellar spacing measured in as-grown and crept specimen after a constant strain of 5%. The results of Fig. 4 suggest that the distribution curves at

5% strain represent the stationary curves after the completion of parallel twinning. No change in the distribution curve from the underformed state is recognized at 100 MPa. However, the distribution curves obviously shift toward smaller size in the specimens deformed at 200 and 251 MPa. The arithmetical average values of lamellar spacing are plotted against the applied stress in Fig. 7. The lamellar spacing decreases with increasing applied stress at stresses higher than 126 MPa. At 251 MPa, for example, the lamellar spacing at 100 MPa remains at the original value, suggesting a critical stress for parallel twinning of 120 MPa in the present PST crystal.

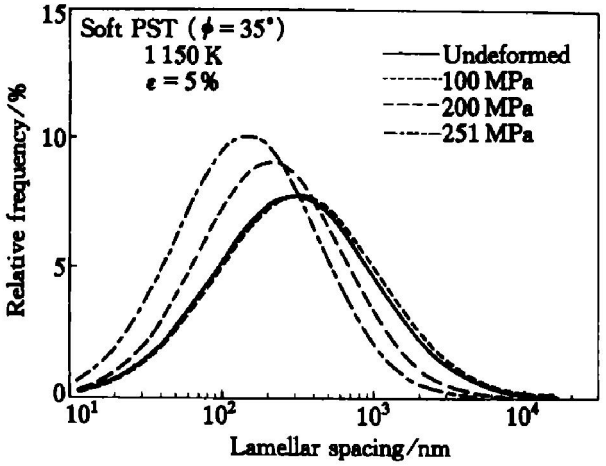

Fig. 6 Distribution curves of lamellar spacing measured after 5% deformation at each creep stress against creep strain

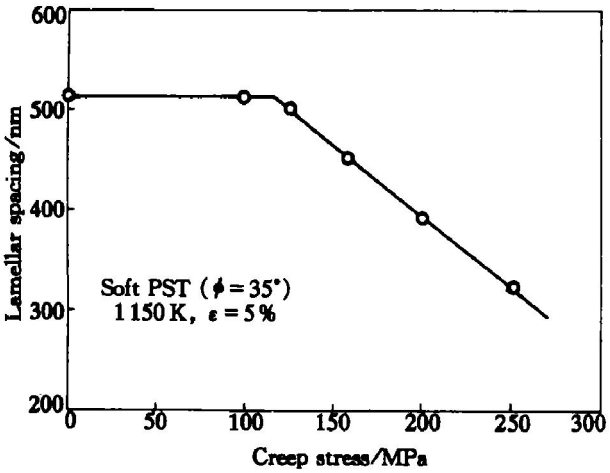

Fig. 7 Lamellar spacing λ^* measured after completion of parallel twinning as a function of applied creep stress σ

By using the Schmid factor for the $[\bar{1}\bar{1}2](111)$ parallel twinning (0.407), the critical resolved shear stress (CRSS) for twinning is calculated to be 50 MPa in the Ti-48% Al alloy at 1 150 K. This value is smaller than that measured by high strain rate deformation: 151 MPa in Ti-49.3% Al (mole fraction) at 3 000 s^{-1} and 1 073 K. This difference suggests that stress concentration created by dislocation motion during creep may assist the nucleation of the parallel twins.

3.5 Saturation level of lamellar spacing

It is obvious from Fig. 7 that the number of parallel twins that can be added to a lamellar structure increases with increasing applied stress. The coherency stress in a lamellar structure[28, 29] and the interfacial energy per unit volume increase with decreasing lamellar spacing. Therefore, the stress necessary to nucleate parallel twins should increase with decreasing lamellar spacing. In other words, there should be a minimum lamellar spacing λ_T^* attainable by parallel twinning at an applied stress τ. The value of λ_T^* may be related to τ by the following equation:

$$\lambda_T^* = \alpha Gb/\tau \tag{5}$$

where G is the shear modulus, b is the magnitude of Burgers vector, and α is a constant. The actual number of boundaries added by parallel twinning in the domains III_M and II_T is three times larger than the average value defined by Eqn. (1), since parallel twinning occurs in the two orientation variants of γ domain only. Eqn. (1) is modified to the following form, using the actual value of lamellar spacing λ_T in the twinning domains:

$$\frac{1}{\lambda_T} = \frac{1}{\lambda_0} + 6n \tag{6}$$

From Eqns. (5) and (6), the number of parallel twins n^* that can be added at a stress τ is given by

$$n^* = \frac{1}{6}\left(\frac{\tau}{\alpha Gb} - \frac{1}{\lambda_0}\right) \tag{7}$$

Substituting this equation into Eqn. (1), the average lamellar spacing λ^* after the completion of parallel twinning is obtained as

$$\frac{1}{\lambda^*} = \frac{2}{3}\frac{1}{\lambda_0} + \frac{m}{3\alpha Gb}\sigma \tag{8}$$

where m is the Schmid factor. This equation gives the average lamellar spacing after the completion of parallel twinning at applied creep stress σ.

Eqn. (8) predicts a linear relation between the reciprocal value of λ^* and applied creep stress. In Fig. 8, the values of lamellar spacing measured at 5% strain, that correspond to λ^*, are plotted against creep stress according to Eqn. (8). Several assumptions were made to derive the equation as mentioned above. The linear stress dependence of $(1/\lambda^*)$ above 126 MPa confirms the assumptions to be correct. The slope of the straight line in Fig. 8 is calculated to be 9×10^{-3} $(\mu m \cdot MPa)^{-1}$. For the $1/6[\bar{1}\bar{1}2](111)$ parallel twinning in domain III_M and II_T, $m = 0.407$, $b = 0.16$ nm, and $G = 60$ GPa at 1 150 K. The value of α is estimated at 1.6 on the basis of these quantities.

3.6 Effect of initial lamellar spacing

The lamellar spacings measured after the comple-

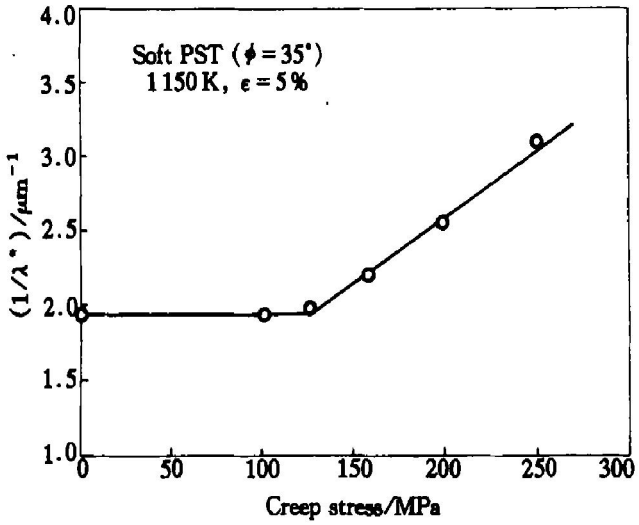

Fig. 8 Change of $1/\lambda^*$ with creep stress σ

tion of parallel twinning are compared in Fig. 9 between the PST crystals having the different initial lamellar spacings: λ_0 = 300 nm and 870 nm. The peak value of distribution curve of lamellar spacing is used in the comparison. The arithmetical average value and the peak value of the present PST crystal are 513 nm and 300 nm, respectively. The experimental results of the other crystal have been reported in Ref. [17]. Both materials show similar behavior: the parallel twinning is inactive below a critical stress of about 120 MPa, and the lamellar spacing measured after creep tests decreases with increasing creep stress. It is noted that the refinement of lamellar spacing is more substantial in the coarse lamellar material. The lamellar spacing attainable by parallel twinning at the high creep stress seems independent of the initial lamellar spacing.

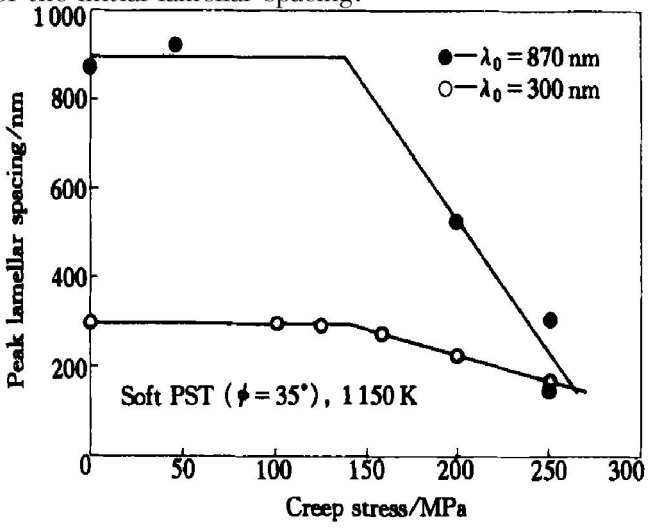

Fig. 9 Influence of initial lamellar spacing on peak values of lamellar spacing measured after completion of parallel twinning against creep strain

3.7 Effect of lamellar refinement on creep behavior

The normal transient creep curves were always recorded in creep of the soft-oriented PST crystal. The creep curves are drawn in Fig. 10 in the form of creep rate as a function of creep strain. The creep rate decreases monotonously to a stationary value with the progress of creep deformation. The change in creep rate is a little after 2% strain. The creep rate at 5% strain is plotted against creep stress in Fig. 11. At this strain, the lamellar spacing is refined by parallel twinning at stresses higher than 120 MPa, while it remains at the original spacing at lower stresses. The figure exhibits an identical stress exponent over the whole stress range investigated regardless of the activity of parallel twinning. The stress exponent of 3.8 is typical of dislocation creep in single-phase materials.

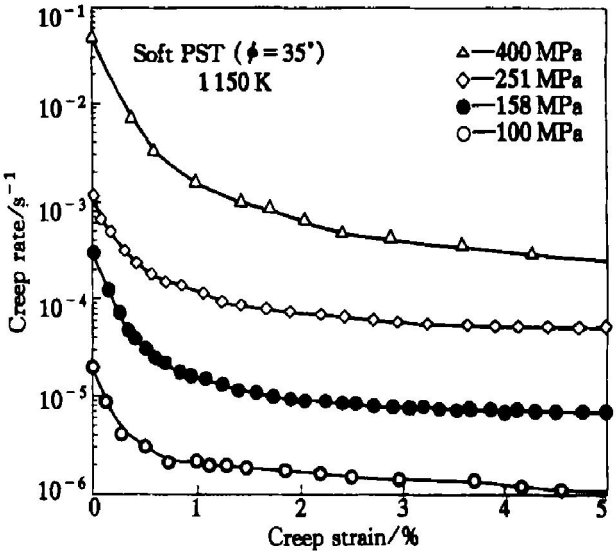

Fig. 10 Effect of applied stress on creep curves of soft-orientated PST crystals

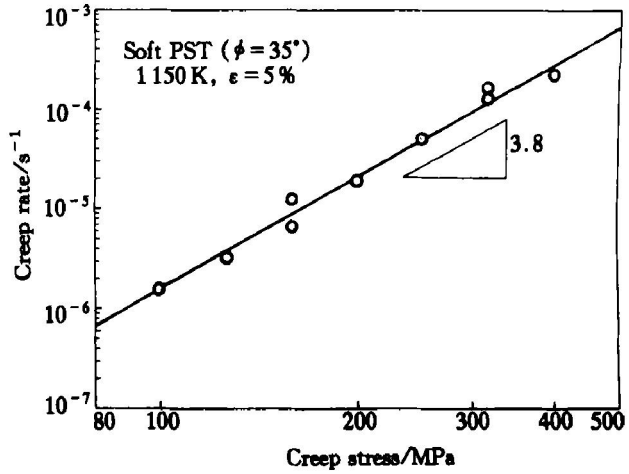

Fig. 11 Stress dependence of creep rate measured at 5% strain in soft-orientated PST crystals

The parallel twinning refines lamellar microstructure, and introduces additional barrier to hard mode deformation. In polycrystals, the hard mode deformation is necessary to maintain strain compatibility. It has been proved in polycrystalline TiAl alloys that creep resistance of lamellar microstructure

increases with decreasing lamellar spacing[9, 10]. Seo et al[26] also have pointed out on a polycrystalline material that the lamellar refinement makes a harder microstructure and consequently provide a greater creep resistance. However, no change in stress exponent is detected in Fig. 11 regardless of the activity of parallel twinning. It is suggested that the hardening effect of parallel twinning is hidden by some special situation in the soft-orientated PST crystal. Deformation of the soft PST crystal is dominated by the soft deformation modes whose slip planes are parallel to lamellar boundaries[17]. Thus, the refinement of lamellar spacing is not effective to hinder the motion of soft mode dislocation. There are six orientation variants of lamellae, and the parallel twinning occurs in the domains III_M and II_T in compression tests. After the parallel twinning, the twinned domains become domains III_T and II_M, respectively. However, the Schmid factors for the soft deformation modes ($1/2\langle 1\bar{1}0\rangle$ and $1/2[\bar{1}\bar{1}2]$ on (111)) do not change after twinning (as shown in Table 1). As a result, the parallel twinning cannot contribute to hardening in the soft-oriented PST crystal.

4 CONCLUSIONS

1) Parallel twinning occurs in the early stage of creep deformation in the lamellae favorably oriented for parallel twinning. The parallel twinning creates most of the creep strain in the twinning domains. However, the parallel twinning finishes after a strain of 3% at creep stress of 251 MPa at 1 150 K.

2) Parallel twinning reduces average lamellar spacing. The minimum lamellar spacing attainable by parallel twinning decreases with increasing applied stress. The activity of parallel twinning is more significant in a coarse lamellar material.

3) There is a critical resolved shear stress for parallel twinning and it is estimated to be 50 MPa in a Ti-48% Al PST crystal at 1 150 K.

4) The stress exponent for creep rate is identical regardless of the activity of parallel twinning. The lamellar refinement by parallel twinning cannot contribute to hardening because of the special situation of the soft-orientated PST crystal in which the primary slip planes are parallel to the lamellar boundaries.

ACKNOWLEDGEMENTS

The present research was supported by JSPS (Cooperative Research Project between Japan and US) and the Ministry of Education, Science, Sports and Culture, Japan (No. 11450259 and 13555182). The material used was kindly provided by Prof. Yamaguchi and Dr. Inui at Kyoto University.

[REFERENCES]

[1] Kim Y W. Ordered intermetallic alloys part III: gamma titanium aluminides [J]. J Metals, 1994, 46: 30– 39.

[2] Beddoes J, Wallace W, Zhao L. Current understanding of creep behavior of near gamma-titanium aluminides [J]. Intern Mater Rev, 1995, 40: 197– 217.

[3] Liu C T, Schneibel J H, Wright J L, et al. Tensile properties and fracture toughness of TiAl alloys with controlled microstructure [J]. Intermetallics, 1996, 4: 429 – 440.

[4] Maziasz P J, Liu C T. Development of ultrafine lamellar structures in two-phase γ-TiAl alloys [J]. Metall Mater Trans A, 1998, 29: 105– 117.

[5] Liu C T, Maziasz P J. Microstructural control and mechanical properties of dual-phase TiAl alloys [J]. Intermetallics, 1998, 6: 653– 661.

[6] Wroth B D, Jones J W, Allison J E. Creep deformation in near γ-TiAl part Ⅰ: the influence of microstructure on creep deformation in Ti-49Al-1V [J]. Metall Mater Trans A, 1995, 36: 2947– 2959.

[7] Es-Souni M, Bartels A, Wagner R. Creep behaviour of a fully transformed near γ-TiAl alloy Ti-48Al-2Cr [J]. Acta Metall Mater, 1995, 43: 153– 161.

[8] Morris M A, Lipe T. Creep deformation of duplex and lamellar TiAl alloys [J]. Intermetallics, 1997, 5: 329– 337.

[9] Maruyama K, Yamamoto R, Nakakuki H, et al. Effect of lamellar spacing, volume, fraction and grain size on creep strength of fully lamellar TiAl alloys [J]. Mater Sci Eng, 1998, A239/240: 419– 428.

[10] Maruyama K, Kim H Y, Luzzi D E. Proceedings of the Third International Symposium on Structural Intermetallics [C]. TMS, Warrendale, PA, 2001.

[11] Appel F, Wagner R. Transgranular cleavage fracture of Fe_3Al intermetallics induced by moisture and aqueous environments [J]. Mater Sci Eng, 1998, R22: 187– 195.

[12] Yamaguchi M, Umakoshi Y. The deformation behaviour of intermetallic superlattice compounds [J]. Prog Mater Sci, 1990, 14: 1– 148.

[13] Inui H, Kishida K, Misaki M, et al. Temperature dependence of yield stress, tensile elongation and deformation structures in polysynthetically twinned crystals of Ti-Al [J]. Phil Mag A, 1995, 72: 1609– 1631.

[14] Skrotzki B, Unal M, Eggeler G. On the role mechanical twinning in creep a near γ-TiAl alloy with duplex microstructure [J]. Scripta Mater, 1998, 39: 1023– 1029.

[15] Imayev R M, Imayev V M, Salishchev G A. Formation of submicrocrystalline structure in TiAl intermetallic compound [J]. J Mater Sci, 1992, 27: 4465– 4471.

[16] Wegmann G, Maruyama K. On the microstructural stability of TiAl/Ti_3Al polysynthetically twinned crystals under creep conditions [J]. Phil Mag A, 2000, 80: 2283– 2298.

[17] Wegmann G, Suda T, Maruyama K. Deformation characteristics of polysynthetically twinned (PST) crystals during creep at 1 150 K [J]. Intermetallics, 2000,

8: 165- 177.

[18] Yoo H M. Twinning and mechanical behavior titanium aluminides and other intermetallics [J]. Intermetallics, 1998, 6: 597- 602.

[19] Morris M A, Leboeuf M. Deformed microstructure during creep of TiAl alloys: role of mechanical twinning [J]. Intermetallics, 1997, 5: 339- 354.

[20] Jin Z, Bieler T R. An in-situ observation of mechanical twin nucleation and propagation in TiAl [J]. Phil Mag A, 1995, 71: 925- 947.

[21] Farenc S, Coujou A, Couret A. An in-situ study of twin propagation in TiAl [J]. Phil Mag A, 1993, 67: 127 - 142.

[22] Zin Z, Chong S W, Bieler T R. Gaman Titanium Aluminides [C]. Kim Y W, Wagner R, Yamaguchi M ed. TMS, Warrendale, PA, 1995, 975.

[23] Gray G T. Twinning in Advanced Materials [C]. Yoo M H, Mutig M, TMS ed. Warrendale, PA, 1994, 337.

[24] Kim H Y, Maruyama K. Parallel twinning during creep deformation in soft orientation PST crystal of TiAl alloy [J]. Acta Mater, 2001, 49: 2635- 2643.

[25] Kim H Y, Maruyama K. Deformation structure during creep deformation in soft orientation PST crystals [J]. Intermetallic, 2001, 9: 929- 935.

[26] Seo D Y, Bieler T R, An S U, et al. Changes in microstructure during primary creep of a Ti-47Al-2Nb-1Mn-0. 5W-0. 5Mo-0. 2Si alloy [J]. Metall Mater Trans A, 1998, 29A: 89- 104.

[27] Seo D Y, An S U, Bieler T R, et al. Gamma Titanium Aluminides [C]. Kim Y W, Wgner R, Yamaguchi M ed. TMS, Warrendale, PA, 1995, 745.

[28] Hazzledine P M. Coherency and loss of coherency in lamellar Ti-Al [J]. Intermetallics, 1998, 6: 673 - 677.

[29] Grinfeld M A, Hazzledine P M, Shoykhet B, et al. Coherency stresses in lamellar Ti-Al [J]. Metall Mater Trans A, 1998, 29A: 937- 942.

(Edited by YANG Bing)